

Reviews

Prognostic Implications and Immune Infiltration in the Nod-like receptor signaling pathway: A Comprehensive Analysis across Pan-cancer

DIO: <https://dx.doi.org/10.71373/ZAGA8611>

Submitted 2 October 2024

Accepted 26 October 2024

Published 10 November 2025

Qiuxia Meng, #1 Tengcheng Que, #2,3,4 Tengyue Yan, 5 Zengjing Liu, 1 Huilin Wei, 6 Bo Xie, 1 Boying Liang, 7 Wen Li, 6,8 Die Zhang, 5 Nili Jiang, 6 Huifeng Wang, 9 Wenjian Liu, ✉2 and Yanling Hu, ✉1,2,6

Purpose: Nucleotide-binding oligosaccharide-like receptors (NOD) are pivotal molecules with crucial roles in the regulation of inflammation, tumor transformation, angiogenesis, tumor stem cells, and chemoresistance. This study aimed to assess the prognostic implications of NOD signaling in diverse cancer types and its relationship with immune infiltration. **Methods:** Gene expression data from TCGA related to the NOD signaling pathway were integrated with clinical data. Prognostically relevant NOD pathway genes were analyzed using univariate and multivariate Cox regression and Kaplan-Meier survival analysis. The accuracy of our prediction model was validated through receiver operating characteristic (ROC) curve analysis. Single-cell analysis of genes associated with reduced survival in patients, and single-sample immunoinfiltration analysis revealed cell-level differences between different groups. **Results:** Univariate Cox regression analysis, multivariate Cox regression analysis and Kaplan-Meier analysis were used to identify prognostic genes in NOD pathway. TRAF5 is an important prognostic gene in multiple cancer types, and mutation analysis showed that patients with TRAF5 mutations had reduced survival. Immune infiltration analysis revealed differences in effector memory CD8 T cells and immature B cells between high- and low-risk groups, suggesting potential druggable targets. Single-cell analysis highlighted that reduced survival was associated with overexpression of TXN in both primary and metastatic tissues. **Conclusion:** NOD signaling pathway, specifically TRAF5, plays a critical role in cancer prognosis across various cancer types. Immune infiltration disparities offer therapeutic opportunities, and TXN represents a promising target for novel anticancer treatments.

Introduction

Cancer represents a prevalent and substantial component of the global health landscape, with the incidence and mortality rates steadily rising year after year [1]. Notably, breast, lung, colorectal, prostate, and gastric cancers stand as prominent malignancies on a worldwide scale, contributing significantly to the ever-increasing global cancer burden, which is projected to reach a staggering 28.4 million cases by 2040 [1]. Contemporary therapeutic approaches for various cancers encompass surgical resection, radiotherapy, chemotherapy, and targeted therapy, yet multiple challenges persist within the therapeutic landscape [2]. Concurrently, cancer ranks as the second leading cause of death on a global scale, and it imposes a substantial

economic burden, particularly in our nation [3,4]. Consequently, a pressing need emerges for comprehensive investigations into cancer's prognostic factors, aiming to guide clinical interventions and enhance patient survival.

Nod-like receptors (NLRs) occupy a pivotal role in the recognition of a broad spectrum of pathogens, instigating innate immune responses by orchestrating the activation of the NF κ B and MAPK pathways. This activation cascade ultimately culminates in the production of cytokines and the induction of apoptosis [5,6]. Notably, the oligomerization of NLRs, exemplified by pattern recognition receptors like NLRP1 and NLRP3, results in the assembly of multiprotein complexes, subsequently triggering Caspase-1 activation. This, in turn, leads to the emergence of the inflammatory cytokines IL-1 β and IL-18, which are implicated in cell death [7,8,9,10]. Importantly, this phenomenon is associated with the invasive growth of malignancies such as breast, gastric, lung, and skin cancers [11,12].

Recognizing the pivotal role of NLRs in the regulation of immune responses and inflammation, it becomes paramount to elucidate the impact of the NLR signaling pathway on cancer. In recent years, several investigations have indicated, through KEGG functional analysis, that the genes relevant to cancer in breast, pancreatic adenocarcinoma, and glioblastoma multiforme (GBM) are predominantly enriched in the Nod-like receptor signaling pathway [13,14,15]. Nevertheless, the current comprehension of NLRs in the context of pan-cancer and the underlying mechanisms of their signaling pathway remains limited. Consequently, it becomes imperative to embark on further explorations

1 Information and Management College of Guangxi Medical University, Nanning 530021, Guangxi, China. 2 Faculty of Data Science, City University of Macau, 999078 Macau, China. 3 Guangxi Forestry Research Institute, 530002, Nanning, Guangxi, China. 4 School of Basic Medical Sciences, Youjiang Medical University for Nationalities, 533000, Baise, Guangxi, China. 5 Collaborative Innovation Centre of Regenerative Medicine and Medical BioResource Development and Application Co-constructed by the Province and Ministry of Guangxi Medical University, Nanning 530021, Guangxi, China. 6 Life Sciences College of Guangxi Medical University, Nanning 530021, Guangxi, China. 7 Department of Immunology, School of Basic Medical Sciences, Guangxi Medical University, Nanning, China. 8 Department of Biochemistry and Molecular Biology, School of Basic Medicine, Guangxi Medical University, Nanning, Guangxi, China. 9 Department of Human Anatomy, School of Basic Medical Sciences, Guangxi Medical University, Nanning, Guangxi, China.

Yanling Hu, Email: ylhupost@163.com.

Wenjian Liu, Email: andylau@cityu.mo.

✉Corresponding author.

#Contributed equally.

n of NLRs, with the aim of fostering innovative perspectives and methodologies for cancer treatment and prognostic evaluation on a pan-cancer scale.

In this study, we screened and analyzed genes associated with the NLRs signaling pathway based on gene expression data and clinical data from the Cancer Genome Atlas (TCGA) dataset to assess the prognostic value of these genes in pan-cancer. Subsequently, we also performed immune cell infiltration analysis, mutation analysis, and single cell analysis to fully investigate the pan-carcinoma situation.

2 Methods

2.1 Data collection and processing

Nod-like receptor signaling pathway genes were obtained from the KEGG database (<https://www.genome.jp/kegg/>), totaling 184 genes (Table S1). After excluding cancers with limited sample cases or those lacking normal sample controls, gene expression matrices for both normal and diseased samples for 10 cancer types were acquired from the Cancer Genome Atlas (TCGA). Additionally, clinical data, including patient gender, age, survival status, pathological stage, and survival period, were collected. The 10 cancer types encompassed Bladder Urothelial Carcinoma (BLCA), Breast Invasive Carcinoma (BRCA), Colon Adenocarcinoma (COAD), Esophageal Carcinoma (ESCA), Glioblastoma Multiforme (GBM), Head and Neck Squamous Cell Carcinoma (HNSC), Lung Adenocarcinoma (LUAD), Lung Squamous Cell Carcinoma (LUSC), Rectum Adenocarcinoma (READ), and Stomach Adenocarcinoma (STAD). Table S2 lists the full names, tumor samples, normal samples and total samples of the ten cancers. Subsequently, the data underwent thorough cleaning and preprocessing to eliminate samples with missing critical information, ensuring the availability of a sample collection for each cancer type for subsequent analysis.

2.2 Identification of Differentially Expressed Genes

For the analysis of Nod-like receptor pathway genes, we employed the "edgeR" R package to identify differentially expressed genes between normal and tumor samples. The criteria for screening were set as $|\log_2 \text{fold change (FC)}| > 1$ and a false discovery rate (FDR) of < 0.05 .

2.3 Univariate and Multivariate Cox Regression Analysis

We performed univariate Cox regression analyses using the "survival" software package to assess the relationship between each gene and patient survival[16,17]. The upper and lower limits of the corresponding hazard ratio (HR) and 95% confidence intervals (HR95H, HR95L) are calculated. Risk score $HR > 1$ indicates that the expression level of this gene is negatively correlated with the prognosis, t

hat is, the higher the expression level, the worse the prognosis; $HR < 1$ indicates that the expression level of this gene is positively correlated with the prognosis, that is, the higher the expression level, the better the prognosis; $HR = 1$ indicates that the gene is not associated with prognosis. Subsequently, the "glmnet", "survival" and "survminer" packages were used to conduct multivariate cox regression analysis[18], establish the prognosis model, and calculate the sample risk score.

2.4 Mapping Survival and Risk Curves

The risk scores for patients across the 10 cancer types were computed using the risk score formula derived from the prognostic model. Subsequently, patients were stratified into high-risk and low-risk groups. To investigate the connection between risk scores and overall survival, a log-rank test was conducted for each cancer type employing the "survival" software package. Statistical significance was defined as p-values less than 0.05.

Moreover, risk curves and heat maps were generated using the "pheatmap" software package to further explore the relationship between risk scores and survival outcomes[19,20].

2.5 Independent Prognostic Analysis

In the independent prognostic analysis, the risk score derived from the prognostic prediction model was employed as a predictor variable, while other clinical factors were included as covariates. This analysis was conducted to evaluate the independent prognostic predictive capability of the risk score. The predictive performance of the risk score for patient survival, in consideration of other factors, was assessed by calculating the hazard ratio (HR) and its corresponding 95% confidence interval (HR95H, HR95L).

2.6 Construction of ROC curves and nomograms

Receiver Operating Characteristic (ROC) curves were constructed using the "survival," "survminer," and "timeROC" software packages to evaluate the predictive performance over time. The Area Under the Curve (AUC) was utilized to illustrate the accuracy of predictions. A higher AUC value indicates that the corresponding ROC curve is closer to the upper-left corner, signifying a higher true positive rate and a lower false positive rate. In essence, a higher AUC value corresponds to greater prediction accuracy [21,22].

The nomogram is a clinical prediction tool that leverages the outcomes of multivariate Cox regression analysis[23].

It amalgamates the associations of multiple variables to visually represent the impact of each variable on the prognosis. The nomogram assigns scores to the range of values for each of the selected clinical factors in the model, based on their respective influence on the final outcome variable. When predicting an individual sample, the scores for each influencing factor can be summed to yield a total score. The relationship between the total score and th

e probability of the outcome event is then utilized to diagnose or predict the onset and progression of the disease, thus furnishing the predictive value of the individual outcome event.

2.7Single-Sample Immunoinfiltration Analysis

To evaluate the correlation between gene expression and the abundance of eight distinct types of immune-infiltration analysis. Subsequently, the ssGSEA algorithm was employed to assess the correlation between the expression of nod-like receptor-related genes and the abundance of immune-infiltrating cells. The data were analyzed on the online tool of HiOmics Cloud Platform (<https://henbio.com/en/tools>)[24].

2.8Mutation Analysis

Further analysis of mutations in nod-like receptor pathway-related genes was conducted using the online platform cBioPortal (<https://www.cbioportal.org/>). This analysis aimed to determine the mutation frequency and mutation types of the selected genes and to explore the association between mutations and prognosis. The findings of the mutation analysis offer valuable insights into the potential functions and repercussions of gene mutations in various cancer species.

2.9Single-Cell Analysis

Datasets for head and neck squamous carcinoma (GSE227156/GSE173468), gastric adenocarcinoma (GSE163558), breast carcinoma (GSE161529), and thyroid carcinoma (GSE184362) were sourced from the GEO database of the National Center for Biotechnology Information (NCBI). These datasets encompassed data from carcinoma in situ (T), metastatic tissue (LN), and paraneoplastic tissue (N). Multi-sample merge analysis on these diverse cancer datasets

was executed utilizing the Seurat R package (version 4.3.0). The data underwent an initial quality control process followed by NormalizeData normalization. Subsequently, highly variable genes were identified, and data normalization was conducted using the ScaleData function. Principal component PCA analysis was employed to reduce the dimensionality of the data. The Harmony function was utilized to mitigate batch effects. Cell projection and clustering analyses were performed using nonlinear dimensionality reduction and the FindClusters function, and cell types were visualized through UMAP analysis. Cell clusters were characterized using the FindAllMarkers function to identify marker genes for each cell cluster. Literature references cited in the dataset were used for cell cluster identification. Bubble plots were generated to illustrate the expression of genes (MAPK9, MAPK10, TXN, TXN2, IFNAR2, CXCL2, IL6, IL1B, IKBKE) in each sample.

ts was executed utilizing the Seurat R package (version 4.3.0).

The data underwent an initial quality control process followed by NormalizeData normalization. Subsequently, highly variable genes were identified, and data normalization was conducted using the ScaleData function. Principal component PCA analysis was employed to reduce the dimensionality of the data. The Harmony function was utilized to mitigate batch effects. Cell projection and clustering analyses were performed using nonlinear dimensionality reduction and the FindClusters function, and cell types were visualized through UMAP analysis. Cell clusters were characterized using the FindAllMarkers function to identify marker genes for each cell cluster. Literature references cited in the dataset were used for cell cluster identification. Bubble plots were generated to illustrate the expression of genes (MAPK9, MAPK10, TXN, TXN2, IFNAR2, CXCL2, IL6, IL1B, IKBKE) in each sample.

Result

Identification of Differentially Expressed Genes

To identify differentially expressed genes between cancerous and normal tissue samples, we used log2FC values obtained from differential analysis to generate heat map (Fig. 1A) and box patterns (Fig. 1B-G). Our analysis revealed differential expression of ANTXR2, CXCL2, ITPR1, GPRC6A, PYDC1, and TXNIP between cancerous lesions and normal tissue samples in multiple cancers.

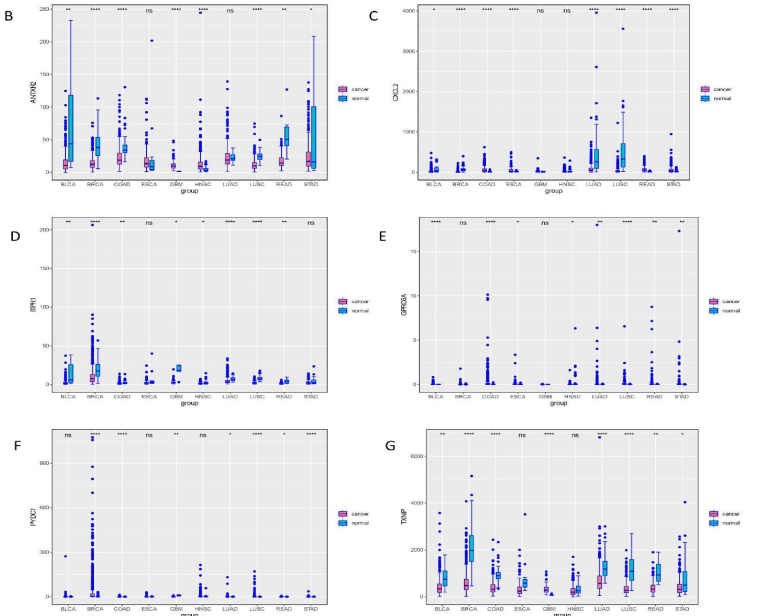
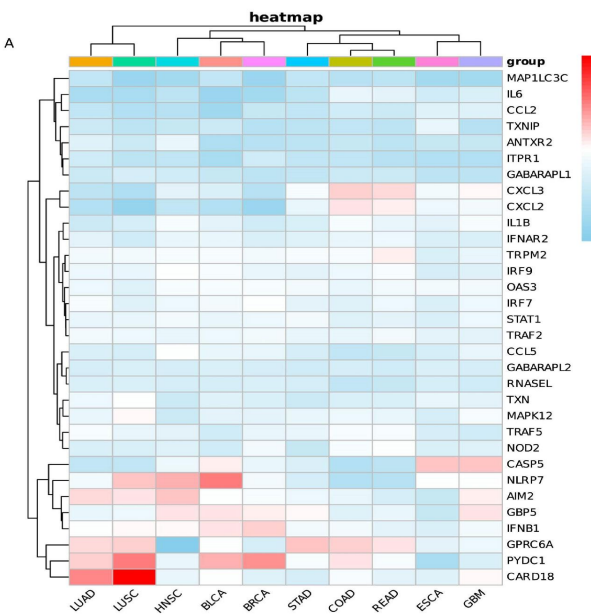


Fig1. Gene expression in different cancer types. (A) Gene expression heat maps in different cancer types. (B) Differential expression of ANTXR2 among different groups. (C) Differential expression of CXCL2 among different groups. (D) Differential expression of ITPR1 among different groups. (E) Differential expression of GPRC6A among different groups. (F) Differential expression of PYDC1 among different groups. (G) Differential expression of TXNIP among different groups.

Prognostic Gene Value in Pan-Cancer

Prognostic genes with relevance to pan-cancer were initially identified through Univariate Cox regression analysis (Table S3). Subsequently, these genes underwent Multivariate Cox regression analysis to pinpoint the most suitable genes for constructing the prognostic risk model (Table S4). Utilizing the risk

scoring formula, the risk score for each sample was computed, and samples were ranked from smallest to largest. Using the median of the risk scores as the threshold value, the samples were categorized into high-expression and low-expression groups. The distribution of differences in survival status and survival time between the high- and low-risk groups was visualized (Fig. 2).

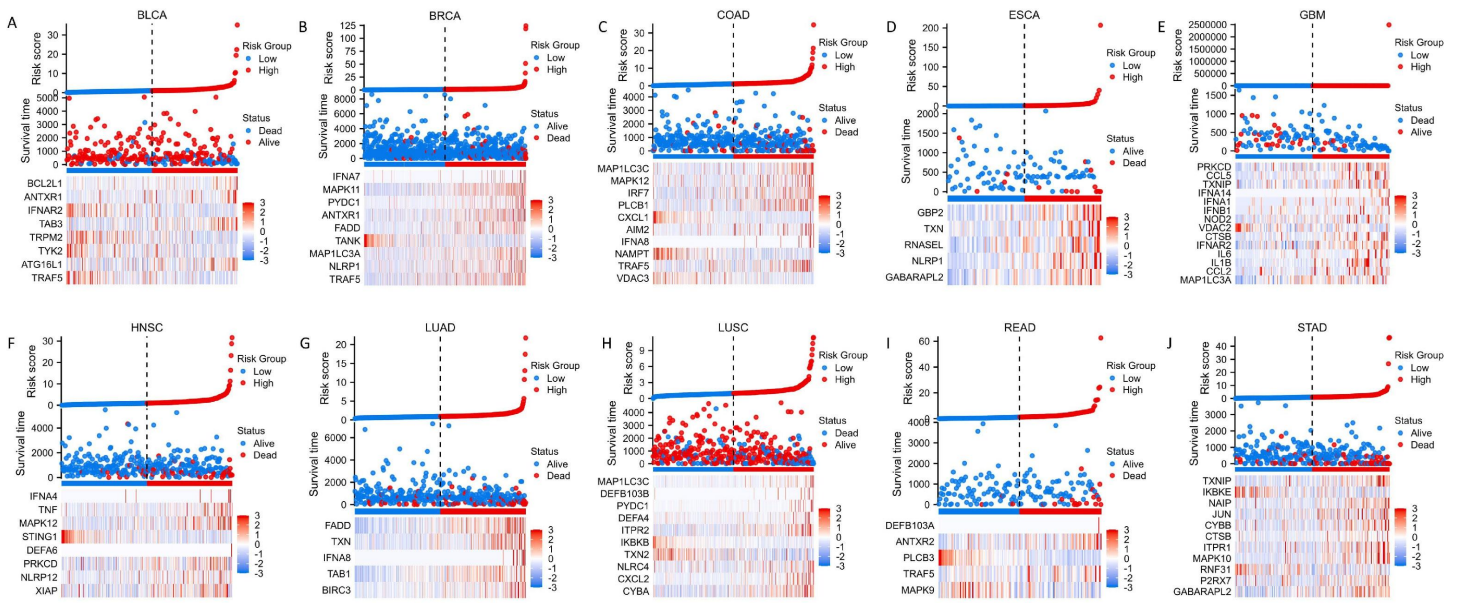


Fig2. Distribution of differences in survival status and survival time between groups for different cancer types. (A) Differences in the distribution of Bladder Urothelial Carcinoma (BLCA) between high and low-risk groups. (B) Differences in the distribution of Breast invasive carcinoma (BRCA) between high and low-risk groups. (C) Differences in the distribution of Colon adenocarcinoma (COAD) between high and low-risk groups. (D) Differences in the distribution of Esophageal carcinoma (ESCA) between high and low-risk groups. (E) Differences in the distribution of Glioblastoma multiforme (GBM) between high and low-risk groups. (F) Differences in the distribution of Head and Neck squamous cell carcinoma (HNSC) between high and low-risk groups. (G) Differences in the distribution of Lung adenocarcinoma (LUAD) between high and low-risk groups. (H) Differences in the distribution of Lung squamous cell carcinoma (LUSC) between high and low-risk groups. (I) Differences in the distribution of Rectum adenocarcinoma (READ) between high and low-risk groups. (J) Differences in the distribution of Stomach adenocarcinoma (STAD) between high and low-risk groups.

The results revealed a significantly higher number of deceased cases in the high-risk region for cancers such as BRCA, COAD, ESCA, HNSC, LUAD, READ, and STAD compared to the low-risk group. Furthermore, the heatmap illustrating the differential expression of prognostic genes between high and low-risk groups demonstrated that all genes associated with a favorable prognosis ($HR < 1$, Table S4) were significantly up-regulated in the low-risk group, while all genes unfavorable to prognosis ($HR > 1$, Table S4) were significantly up-regulated in the high-risk group.

Kaplan-Meier curves (Fig. 3A-J) clearly demonstrated a substantial increase in survival chances for patients in the low-risk group compared to those in the high-risk group across various cancer types, including BLCA ($p < 0.001$), BR

CA ($p < 0.001$), COAD ($p < 0.001$), ESCA ($p = 0.025$), GBM ($p < 0.001$), HNSC ($p < 0.001$), LUAD ($p < 0.001$), LUSC ($p < 0.001$), READ ($p < 0.001$), and STAD ($p < 0.001$). This observation underscored the validity of the risk score as a robust prognostic indicator, with statistical significance defined by $p < 0.05$. Furthermore, time-dependent ROC curves (Fig. 3K-T) were employed to assess the accuracy of the 10 cancer prognosis-related genes in predicting the 1-, 3-, and 5-year overall survival of cancer patients. The area under the curve (AUC) values indicated that the prognostic model exhibited strong predictive capability, thereby identifying the aforementioned prognostic-related genes as valuable prognostic markers for their respective cancer types. In addition, within the pan-cancer prognostic ge

nes, it was noted that TRAF5 was featured in the prognostic genes of BLCA, BRCA, COAD, and READ, while GABARA

PL2 was present in the prognostic genes of ESCA and STAD within the digestive system cancers.

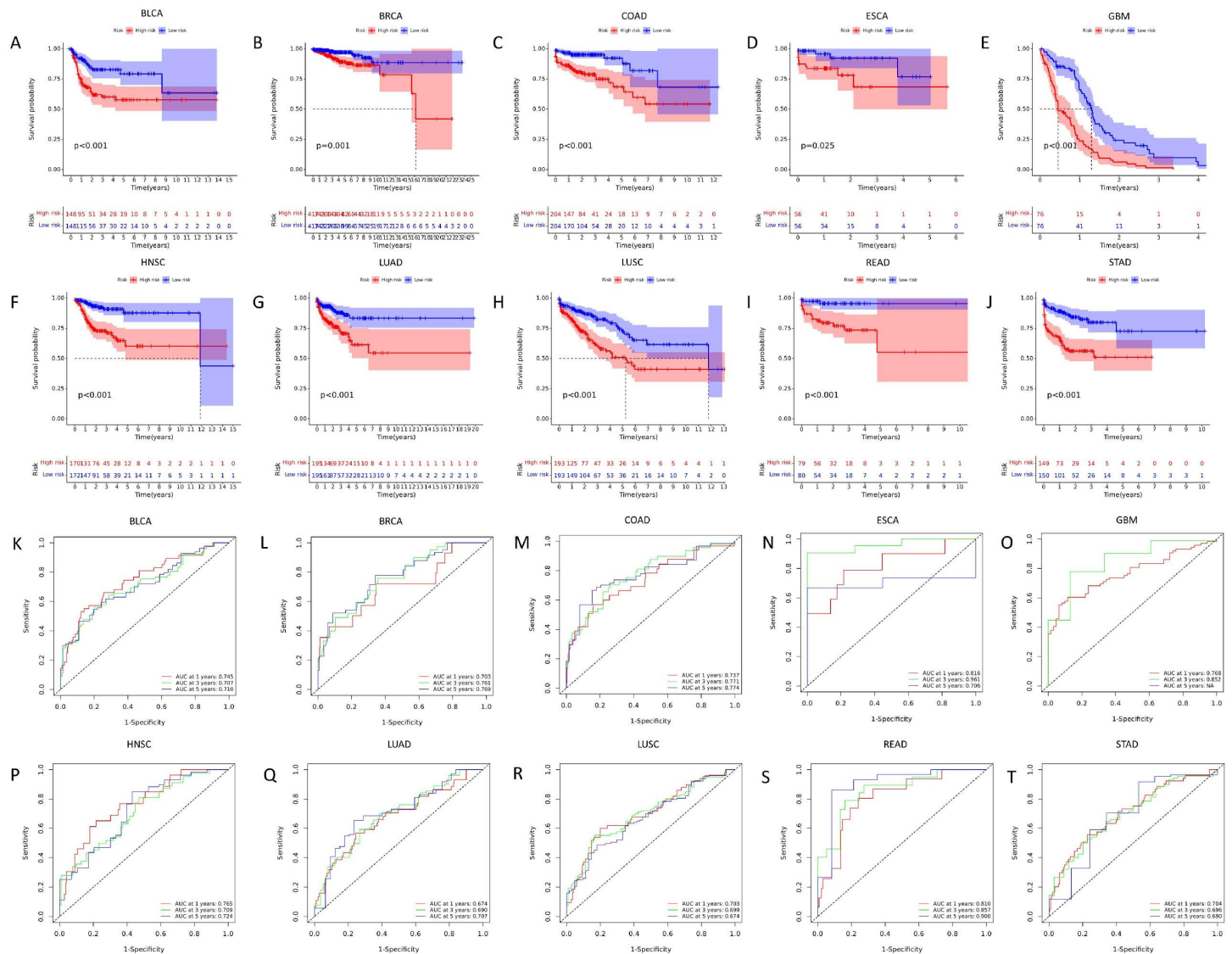


Fig3.Survival probability in different cancer types.(A)Differences in survival probability between groups for Bladder Urothelial Carcinoma (BLCA).(B)Differences in survival probability between groups for Breast invasive carcinoma (BRCA).(C)Differences in survival probability between groups for Colon adenocarcinoma (COAD).(D)Differences in survival probability between groups for Esophageal carcinoma (ESCA).(E)Differences in survival probability between groups for Glioblastoma multiforme (GBM).(F)Differences in survival probability between groups for Head and Neck squamous cell carcinoma (HNSC).(G)Differences in survival probability between groups for Lung adenocarcinoma (LUAD).(H)Differences in survival probability between groups for Lung squamous cell carcinoma (LUSC).(I)Differences in survival probability between groups for Rectum adenocarcinoma (READ).(J)Differences in survival probability between groups for Stomach adenocarcinoma (STAD). (K)-(T) Corresponding ROC curves to validate the accuracy of the survival curves.

Assessment of Independent Prognostic Factors in Patients with 10 Types of Cancer

To gauge whether the risk scores derived from the prognostic prediction model were influenced by other clinical factors, including patient age, gender, and clinical stage, both one-way and multifactor Cox regression analyses were conducted on the risk scores and clinical factors. The results of the univariate Cox regression analysis (Figures S1) demonstrated that the risk scores ($P < 0.001$) could function as independent prognostic factors, independent of o

ther clinical factors, for all cancers except GBM ($P = 0.998$). Importantly, multifactorial Cox regression analysis (Fig. 4A-J) further confirmed that the risk score ($P < 0.001$) was an independent risk factor for these cancers, except for GBM.

Subsequently, time-dependent ROC curve analysis was employed to evaluate the accuracy of the predictive model. The area under the risk score curve (AUC) is as follows: 0.745, 0.703, 0.737, 0.816, 0.704, 0.765, 0.674, 0.703, 0.810 and 0.768 (Fig. 4K-T). These AUC values further underscored the predictive accuracy of the model.

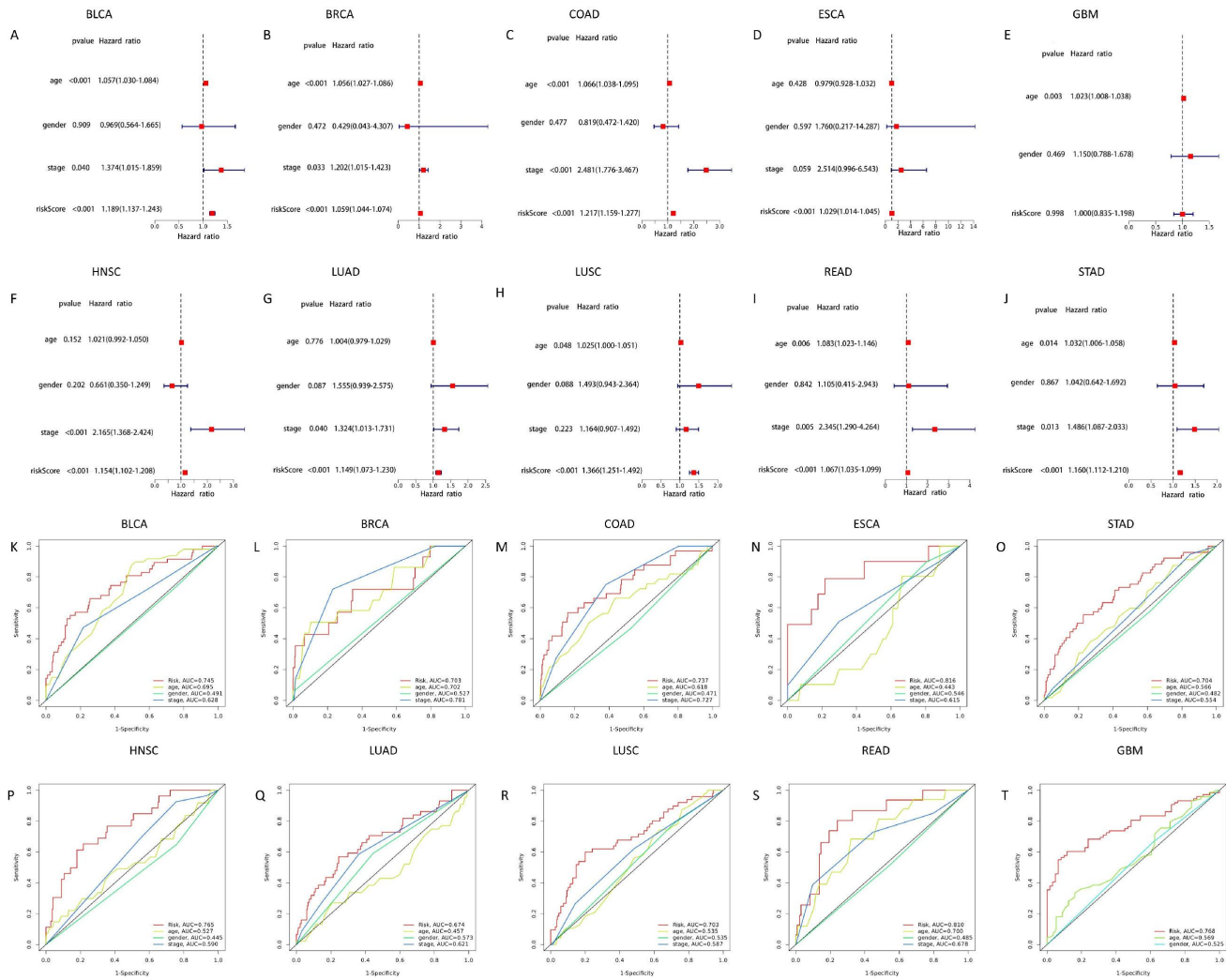


Fig4.Independent prognostic analysis.(A)Multifactor Cox regression analysis for Bladder Urothelial Carcinoma (BLCA).(B)Multifactor Cox regression analysis for Breast invasive carcinoma (BRCA).(C)Multifactor Cox regression analysis for Colon adenocarcinoma (COAD).(D)Multifactor Cox regression analysis for Esophageal carcinoma (ESCA).(E)Multifactor Cox regression analysis for Glioblastoma multiforme (GBM).(F)Multifactor Cox regression analysis for Head and Neck squamous cell carcinoma (HNSC).(G)Multifactor Cox regression analysis for Lung adenocarcinoma (LUAD).(H)Multifactor Cox regression analysis for Lung squamous cell carcinoma (LUSC).(I)Multifactor Cox regression analysis for Rectum adenocarcinoma (READ).(J)Multifactor Cox regression analysis for Stomach adenocarcinoma (STAD). (K)-(T) Corresponding ROC curves to validate the accuracy of the independent prognostic model.

Alignment Diagram (Nomogram)

The alignment diagram, commonly referred to as a nomogram, is constructed based on multifactor regression analysis. It integrates multiple predictors and utilizes line segments with scales plotted on the same plane according to a predefined scale. The length of each line segment represents the range of values that a variable can assume. This graphical representation serves to express the predictive model, incorporating variables such as age, stage, gender, and risk score, which contribute to the magnitude of the outcome event (Fig. 5).

cale. The length of each line segment represents the range of values that a variable can assume. This graphical representation serves to express the predictive model, incorporating variables such as age, stage, gender, and risk score, which contribute to the magnitude of the outcome event (Fig. 5).

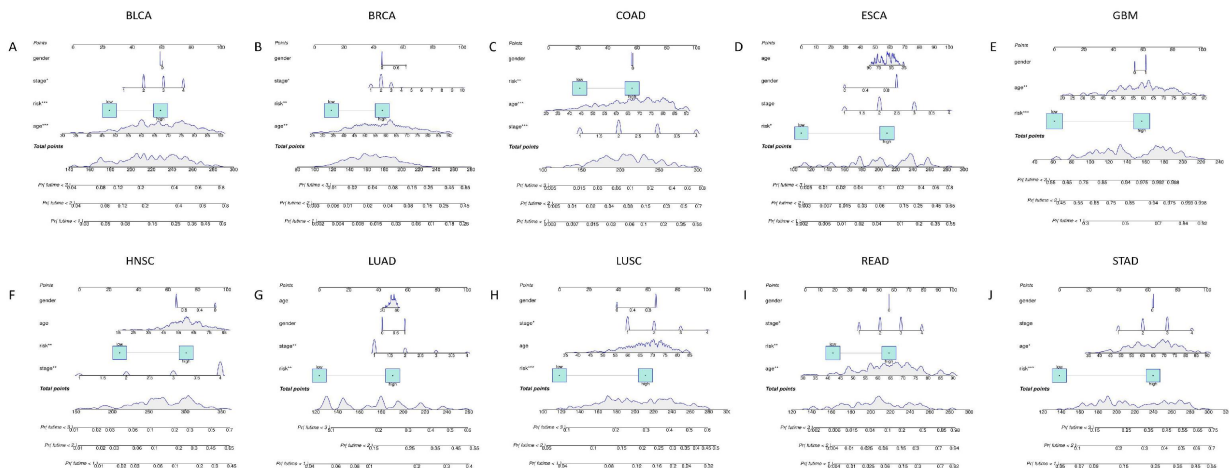


Fig5.Nomogram construction.(A)Construction of nomogram for predicting 1, 2, and 3-year overall survival probability in Bladder Urothelial Carcinoma a (BLCA) based on clinical factors and risk score.(B)Nomogram for Breast invasive carcinoma (BRCA).(C)Nomogram for Colon adenocarcinoma (COAD).(D)Nomogram for Esophageal carcinoma (ESCA).(E)Nomogram for Glioblastoma multiforme (GBM).(F)Nomogram for Head and Neck squamous cell c arcinoma (HNSC).(G)Nomogram for Lung adenocarcinoma (LUAD).(H)Nomogram for Lung squamous cell carcinoma (LUSC).(I)Nomogram for Rectum adenocarcinoma (READ).(J)Nomogram for Stomach adenocarcinoma (STAD).The labels *P<0.05, **P<0.01, ***P<0.001 indicate the statistical significance levels.

In clinical practice, healthcare professionals can employ the column line diagram. They input the actual clinical information of the patient into the diagram, determining the corresponding scores for each variable based on the score scale. These scores are then summed to obtain a total score. This total score

can be placed on the total score scale, and a vertical line can be drawn on the survival rate scale at the corresponding position of the total score scale to estimate the patient's survival rate at 1 year, 2 years, and 3 years.

Analysis of Differences in Immune Cell Infiltration Between Different Samples

Single-sample gene set enrichment analysis (ssGSEA) was utilized to compute the infiltration scores of individual immune cells. The immune infiltration heatmap revealed variations in the levels of specific immune cells. For instance, activated CD4 T cells exhibited higher immune infiltration levels in ESCA and LUSC, with infiltration scores of 0.48 and 0.42, respectively. Conversely, neutrophils demonstrated higher immune infiltration scores in COAD and READ, with scores of 0.65 and 0.37, respectively (Fig. 6A). The analysis of differences in immune cell infiltration between high-risk and low-risk groups uncovered significant disparities. Effector memory CD8 T cells exhibited elevated infiltration

in COAD (p = 8e-05), ESCA (p = 0.0025), HNSC (p = 0.033), LUAD (p = 0.012), READ (p = 0.0047), and STAD (p = 0.00014) when comparing high-risk and low-risk groups (Fig. 6B-K). In these cases, effector memory CD8 T cell infiltration levels were higher in the high-risk groups than in the low-risk groups (Supplemental Fig. 2). Similarly, immature B cells showed variations in infiltration between high-risk and low-risk groups. Specifically, in BRCA (p = 0.03), COAD (p = 0.00016), GBM (p = 0.0058), LUSC (p = 3.7e-09), READ (p = 0.047), and STAD (p = 1.3e-07), statistically significant differences were observed (Fig. 6B-K). Immature B cell infiltration levels were notably higher in the high-risk groups than in the low-risk groups for BRCA, COAD, GBM, LUSC, READ, and STAD (Figures S2)

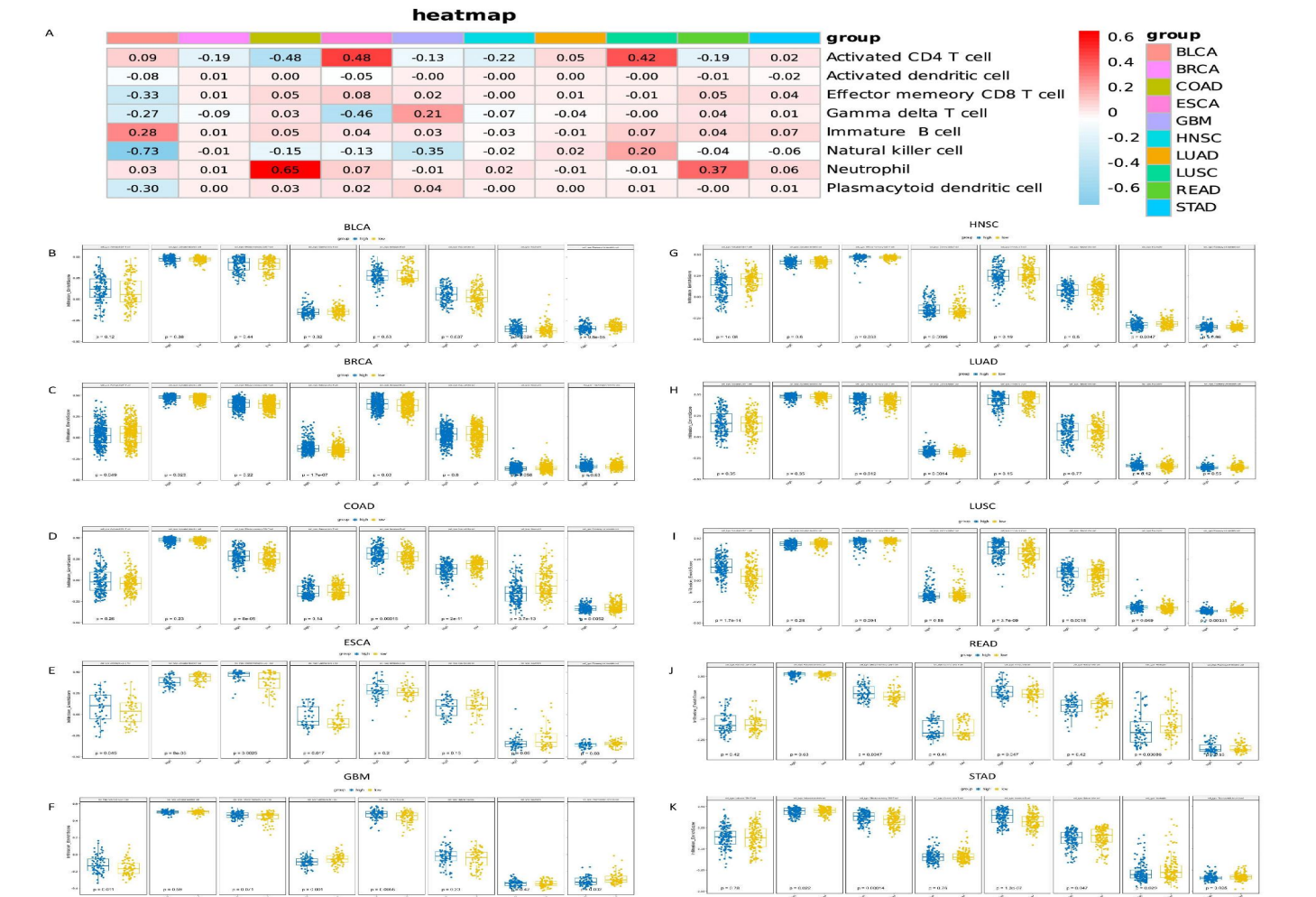


Fig6.Single-sample gene set enrichment analysis and immune cell infiltration.(A)Infiltration scores of immune cells in different cancer ty pes.(B)Differential immune cell infiltration in Bladder Urothelial Carcinoma (BLCA).(C)Differential immune cell infiltration in Breast invasive carcinoma (BRCA).(D)Differential immune cell infiltration in Colon adenocarcinoma (COAD).(E)Differential immune cell infiltration in Eso phageal carcinoma (ESCA).(F)Differential immune cell infiltration in Glioblastoma multiforme (GBM).(G)Differential immune cell infiltratio n in Head and Neck squamous cell carcinoma (HNSC).(H)Differential immune cell infiltration in Lung adenocarcinoma (LUAD).(I)Differenta l immune cell infiltration in Lung squamous cell carcinoma (LUSC).(J)Differential immune cell infiltration in Rectum adenocarcinoma (REA D). (K) Differential immune cell infiltration in Stomach adenocarcinoma (STAD).

Single-cell analysis and mutational analysis of TRAF5 in cancer

The frequency of TRAF5 mutations in the TCGA database was explored using the CBioPortal website, covering data from ten studies encompassing 5667 samples. The findin gs revealed that TRAF5 mutations were present in 3% of patients (Fig. 7A). Notably, copy number variations (CNV) were predominant in BRCA, COAD, ESCA, LUAD, LUSC, and STAD, with CNV occurring in more than 8% of cases in B RCA, although no CNV was observed in READ (Fig. 7B). A comprehensive analysis of mutation sites uncovered a total of 40 mutation sites, comprising 30 missense , 7 truncating, and 3 splice mutations (Fig. 7C). Furthermore, th

e correlation between TRAF5 gene mutations and clinical prognosis was examined. Samples with at least one gene change in mRNA expression were categorized as the alte red group, while those without alterations were designat ed the unaltered group. The results demonstrated signifi cant differences between the two groups in terms of dise ase-specific survival (DSS) ($p = 1.475e-3$), overall survival (OS) ($p = 3.326e-3$), and progression-free survival (PFS) ($p = 1.383e-3$) (Fig. 7D-F). Patients in the altered group exhib ited significantly shorter survival than those in the unalt ered group, indicating that TRAF5 gene mutations were a ssociated with a poorer prognosis regarding DSS, OS, and PFS.

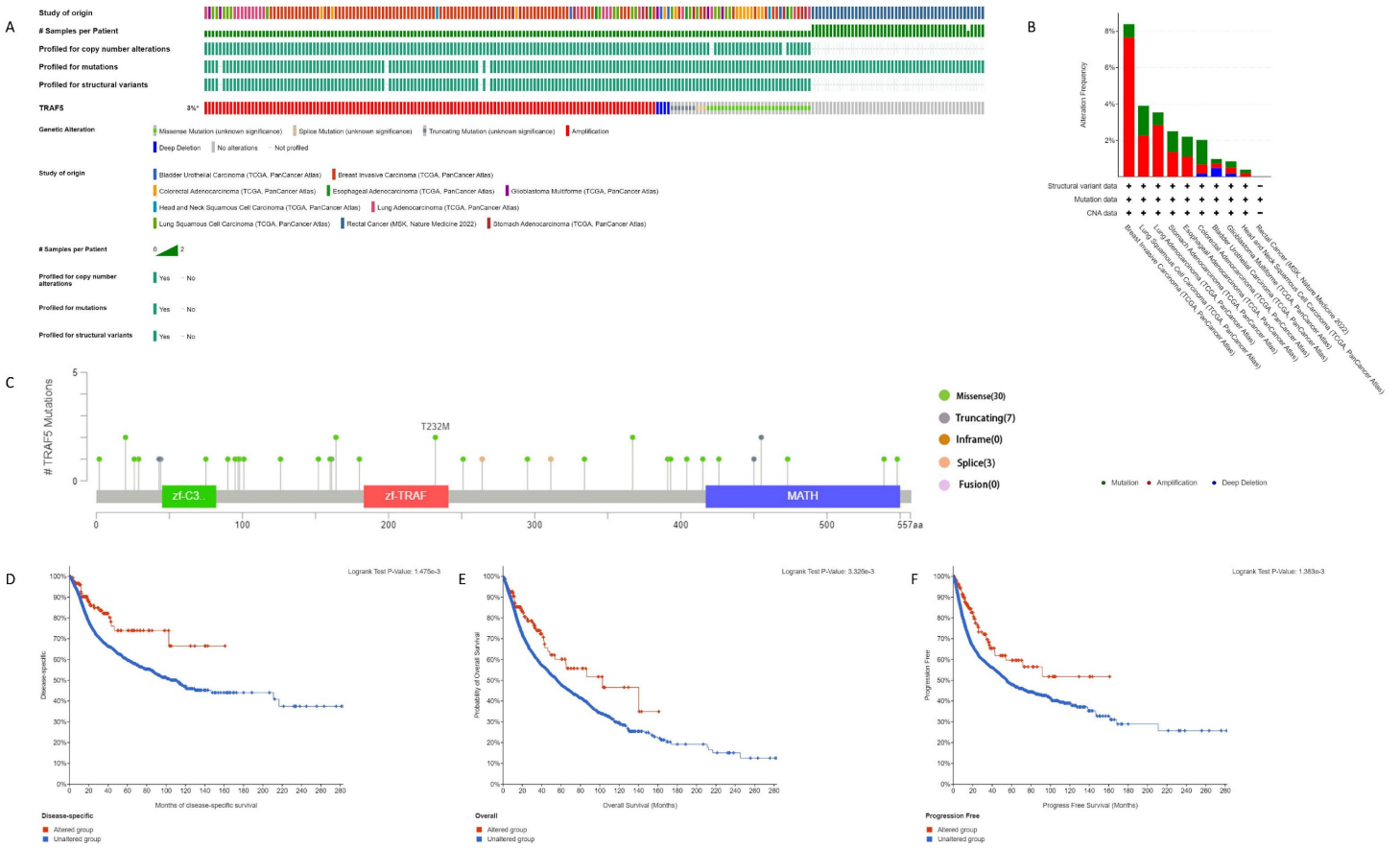
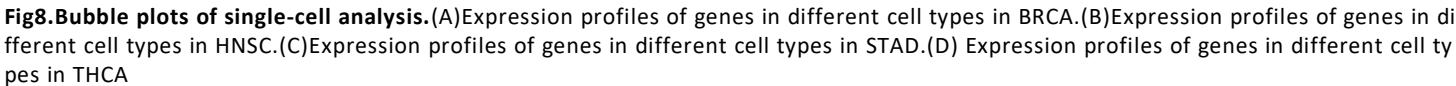


Fig7.Mutational analysis of TRAF5 in different cancer types.(A)OncoPrint of TRAF5 gene alterations in cancer cohorts.(B)Details of TRAF5 gene alteration types in cancer cohorts.(C)Mutational landscape of TRAF5 in different cancer types across protein structural domains.(D) Differences in Disease-Specific Survival (DSS) between two groups.(E)Differences in Overall Survival (OS) between two groups.(F)Differences in Progression-Free Survival (PFS) between two groups.

pes across BRCA, HNSC, STAD, and THCA. Specifically, in HNSC and STAD, CD8+ T cells, epithelial cells, fibroblasts, and macrophages from primary tumor and lymph node metastasis tissues showed elevated expression of TXN, whereas its expression was lower in adjacent non-cancerous tissues. These results provide valuable insights into the complexity of cancer and the underlying biological mechanisms, paving the way for the development of novel therapeutic strategies and potential targets for future cancer treatments.



Discussion

Nucleotide-binding oligomerization domain (NOD)-like receptors, a subset of cytoplasmic pattern-recognition receptors, are integral components of the innate immune system's pathogen pattern-recognition network, alongside RIG-I-like receptors, Toll-like receptors, and the C-type lectin family[25,26]. These receptors serve pivotal roles in governing intracellular responses to infections, noxious agents, and metabolic irregularities[27,28]. Furthermore, NOD-like receptors have emerged as key players in a spectrum of human ailments, encompassing infectious maladies, malignancies, autoimmune disorders, and inflammatory conditions[29,30,31,32,33,34,35]. In the context of cancer, the influence of NOD-like receptors has been notably evident in the development of various malignancies, including but not limited to bladder, colorectal, and colon cancers[29,36,37]. Their regulatory impact on NOD-like receptors is of particular relevance in this regard. Given the relatively understudied nature of the nod-like receptor signaling pathway in pan-cancer contexts, our study embarks on a comprehensive analysis aimed at unveiling the prognostic and immunological relevance of this pathway across various cancers.

In this study, we analyzed gene expression matrices and clinical datasets of 10 cancers (BLCA, BRCA, COAD, ESCA, GBM, HNSC, LUAD, LUSC, READ, STAD) downloaded from TCGA. Univariate and multifactor cox regression analysis showed that TRAF5 had significant prognostic relationship with BLCA, BRCA, COAD and READ. GABARAPL2 has a significant prognostic relationship with ESCA and STAD. According to the risk score formula, the median risk score was taken as the critical value, the samples were divided into high-risk group and low-risk group, and the survival curve and independent prognosis analysis of the high-low risk group were drawn. The results showed that risk score could be used as an independent prognostic factor to predict cancer. Particular emphasis is placed on survival analysis, BLCA, BRCA, COAD, ESCA, GBM, HNSC, LUAD, LUSC, READ, STAD chances of survival in patients with low risk group was obviously higher and high-risk patients. The ROC curve validated the accuracy of our model in predicting 1-year, 3-year, and 5-year overall survival.

In order to further explore the potential role of TRAF5 in cancer prognosis, we used the website cBioPortal for mutation analysis of the TRAF5 gene. The results of the study showed that the proportion of CNV was the highest among BRCA, at more than 8%. In addition, we found that mutations in the TRAF5 gene were significantly associated with poor outcomes (DSS, OS, PFS). These results further confirm the potential role of our prognostic model in determining cancer prognosis. TRAF5 is associated with the occurrence and development of various cancers. For example, TRAF5 promotes the occurrence and development of colon cancer by activating the PI3K/AKT/NF- κ B signaling pathway, and acts as an oncogene[38]. Relevant studies have shown that miR-135a can effectively inhibit gastric cancer (GC) cell metastasis by directly targeting TRAF5 and subsequently inhibiting the NF- κ B pathway, and overexpression of TRAF5 was negatively correlated with the expression of miR-135a in GC tissues[39]. In addition, TRAF5 has been the target of human esophageal squamous carcinoma (ESCC), and miR-26b has tumor suppressive effect on human ESCC through reverse regulation of TRAF5[40]. Overall, our results reveal th

at TRAF5 gene is significantly related to the occurrence and development of cancer, and provide valuable reference for future treatment strategies.

During our single-sample immune cell infiltration analysis, we observed significant differences in multiple immune cells, particularly effector memory CD8 T cells and immature B cells, in the high-risk and low-risk groups for various cancers. Immune cell infiltration within tumors strongly correlates with clinical outcomes, rendering them promising candidates as drug targets to enhance patient survival[41]. Additionally, we conducted a single-cell analysis to delve further into gene expression within various cell types. Notably, the TXN gene exhibited elevated expression across multiple cell types in BRCA, HNSC, STAD, and THCA. Moreover, in the case of HNSC and STAD, the TXN gene demonstrated notably high expression in CD8+T cells, Epithelial cell, fibroblasts and macrophages within the in situ cancer and lymph node metastatic tissues.

Thioredoxin-1 (TXN) assumes a pivotal role in the mitigation of reactive oxygen species, the activation of tumor suppressor genes, and the stimulation of DNA repair enzymes. Numerous studies have reported an overexpression of TXN in solid tumors, a factor significantly associated with an unfavorable prognosis[22]. The gene encoding TXN is classified as a proto-oncogene, a potent driver of tumor growth, and an inhibitor of apoptosis, whether instigated spontaneously or triggered by drug-induced mechanisms[43]. Elevated expression of the TXN gene has been linked to heightened levels of hypoxia-induced factor-1 α (HIF-1 α) and the overexpression of HIF-1 transactivator genes in cancer cells[44,45]. This phenomenon results in increased production of vascular endothelial growth factor and excessive tumor angiogenesis[46]. Furthermore, the overexpression of TXN has demonstrated a strong correlation with aggressive tumor growth and diminished survival among cancer patients[45,46,47]. Notably, Grogan et al[48] localized TXN within tumor cells and noted its overexpression in gastric cancer tissues when compared to normal gastric mucosa. These findings align with our own observations, reinforcing the belief that TXN plays a pivotal role in sustaining the transformed phenotype observed in certain human cancers. Moreover, it contributes to these cancers' resistance to chemotherapy, rendering it a highly promising candidate for cancer drug development[49]. In summary, this comprehensive analysis reveals the prognostic and immunological relevance of NOD-like receptors in various cancers. Particular attention was paid to the potential role of TRAF5 in cancer prognosis. Through in-depth analysis of gene expression and mutation data, we found that TRAF5 is significantly associated with the occurrence and development of multiple cancers and has an important potential role in prognostic judgment. In addition, our immune cell infiltration analysis and single-cell analysis highlight the importance of immune mechanisms in tumor development and point to the key role of the TXN gene in maintaining the cancer transforming phenotype. These findings provide valuable references for future cancer treatment strategies and provide new ideas for further research on the biological mechanisms of cancer.

Reference

1. Sung H, Ferlay J, Siegel RL et al. Global Cancer Statistics 2020: GLOBOCAN Estimates of Incidence and Mortality Worldwide for 36 Cancers in 185 Countries. *CA Cancer J Clin.*2021, 71(3):209-249.doi:10.3322/caac.21660.
2. Yu Z, Gao L, Chen K et al. Nanoparticles: A New Approach to Upgrade Cancer Diagnosis and Treatment. *Nanoscale Res Lett.*2021, 16(1):88.doi:10.1186/s11671-021-03489-z.
3. Collaborators GBDCRF. The global burden of cancer attributable to risk factors, 2010-19: a systematic analysis for the Global Burden of Disease Study 2019. *Lancet.*2022, 400(10352):563-591.doi:10.1016/S0140-6736(22)01438-6.
4. Qiu H, Cao S, Xu R. Cancer incidence, mortality, and burden in China: a time-trend analysis and comparison with the United States and United Kingdom based on the global epidemiological data released in 2020. *Cancer Commun (Lond).*2021, 41(10):1037-1048.doi:10.1002/cac2.12197.
5. Qiu D, Zhang D, Yu Z et al. Bioinformatics approach reveals the critical role of the NOD-like receptor signaling pathway in COVID-19-associated multiple sclerosis syndrome. *J Neural Transm (Vienna).*2022, 129(8):1031-1038.doi:10.1007/s00702-022-02518-0.
6. Fan Z, Pan J, Wang H et al. NOD-like receptor X1, tumor necrosis factor receptor-associated factor 6 and NF- κ B are associated with clinicopathological characteristics in gastric cancer. *Exp Ther Med.*2021, 21(3):208.doi:10.3892/etm.2021.9640.
7. Babamale AO, Chen ST. Nod-like Receptors: Critical Intracellular Sensors for Host Protection and Cell Death in Microbial and Parasitic Infections. *Int J Mol Sci.*2021, 22(21).doi:10.3390/ijms222111398.
8. Huang Y, Xu W, Zhou R. NLRP3 inflammasome activation and cell death. *Cell Mol Immunol.*2021, 18(9):2114-2127.doi:10.1038/s41423-021-00740-6.
9. Moossavi M, Parsamanesh N, Bahrami A et al. Role of the NLRP3 inflammasome in cancer. *Mol Cancer.*2018, 17(1):158.doi:10.1186/s12943-018-0900-3.
10. Platnich JM, Muruve DA. NOD-like receptors and inflammasomes: A review of their canonical and non-canonical signaling pathways. *Arch Biochem Biophys.*2019, 670:4-14.doi:10.1016/j.abb.2019.02.008.
11. Ding Y, Yan Y, Dong Y et al. NLRP3 promotes immune escape by regulating immune checkpoints: A pan-cancer analysis. *Int Immunopharmacol.*2022, 104:108512.doi:10.1016/j.intimp.2021.108512.
12. Voigt C, May P, Gottschlich A et al. Cancer cells induce interleukin-22 production from memory CD4(+) T cells via interleukin-1 to promote tumor growth. *Proc Natl Acad Sci U S A.*2017, 114(49):12994-12999.doi:10.1073/pnas.1705165114.
13. Li C, Zhou Y, Deng H et al. Mining database for the therapeutic targets and prognostic biomarkers among STAT family in glioblastoma. *Cancer Biomark.*2021, 30(2):179-191.doi:10.2233/CBM-201746.
14. Liu B, Huang R, Fu T et al. GBP2 as a potential prognostic biomarker in pancreatic adenocarcinoma. *PeerJ.*2021, 9:e11423.doi:10.7717/peerj.11423.
15. Wu ZH, Tang Y, Yu H et al. The role of ferroptosis in breast cancer patients: a comprehensive analysis. *Cell Death Discov.*2021, 7(1):93.doi:10.1038/s41420-021-00473-5.
16. Lian H, Han YP, Zhang YC et al. Integrative analysis of gene expression and DNA methylation through one-class logistic regression machine learning identifies stemness features in medulloblastoma. *Mol Oncol.*2019, 13(10):2227-2245.doi:10.1002/1878-0261.12557.
17. Yang Z, Liu A, Xiong Q et al. Prognostic value of differentially methylated gene profiles in bladder cancer. *J Cell Physiol.*2019, 234(10):18763-18772.doi:10.1002/jcp.28515.
18. Li L, Liu ZP. Detecting prognostic biomarkers of breast cancer by regularized Cox proportional hazards models. *J Transl Med.*2021, 19(1):514.doi:10.1186/s12967-021-03180-y.
19. Ju M, Bi J, Wei Q et al. Pan-cancer analysis of NLRP3 inflammasome with potential implications in prognosis and immunotherapy in human cancer. *Brief Bioinform.*2021, 22(4).doi:10.1093/bib/bbaa345.
20. Clive AO, Kahan BC, Hooper CE et al. Predicting survival in malignant pleural effusion: development and validation of the LENT prognostic score. *Thorax.*2014, 69(12):1098-1104.doi:10.1136/thoraxjnl-2014-205285.
21. Liu L, Qu J, Dai Y et al. An interactive nomogram based on clinical and molecular signatures to predict prognosis in multiple myeloma patients. *Aging (Albany NY).*2021, 13(14):18442-18463.doi:10.18632/aging.203294.
22. Zhao H, Zhang S, Shao S et al. Identification of a Prognostic 3-Gene Risk Prediction Model for Thyroid Cancer. *Front Endocrinol (Lausanne).*2020, 11:510.doi:10.3389/fendo.2020.00510.
23. Iasonos A, Schrag D, Raj GV et al. How to build and interpret a nomogram for cancer prognosis. *J Clin Oncol.*2008, 26(8):1364-1370.doi:10.1200/JCO.2007.12.9791.
24. Li W, Zhang ZN, Xie B et al. HiOmics: A Cloud-based One-stop Platform for the Comprehensive Analysis of Large-scale Omics Data. *Computational and Structural Biotechnology Journal.*2024, ISSN 2001-0370.doi: <https://doi.org/10.1016/j.csbj.2024.01.002>. (<https://www.sciencedirect.com/science/article/pii/S2001037024000023>).
25. Motta V, Soares F, Sun T et al. NOD-like receptors: versatile cytosolic sentinels. *Physiol Rev.*2015, 95(1):149-178.doi:10.1152/physrev.00009.2014.
26. Kanneganti TD, Lamkanfi M, Núñez G. Intracellular NOD-like receptors in host defense and disease. *Immunity.*2007, 27(4):549-559.doi:10.1016/j.immuni.2007.10.002.
27. Zhong Y, Kinio A, Saleh M. Functions of NOD-Like Receptors in Human Diseases. *Front Immunol.*2013, 4:333.doi:10.3389/fimmu.2013.00333.
28. Hamarsheh S, Zeiser R. NLRP3 Inflammasome Activation in Cancer: A Double-Edged Sword. *Front Immunol.*2020, 11:1444.doi:10.3389/fimmu.2020.01444.
29. Huhn S, da Silva Filho MI, Sanmuganantham T et al. Coding variants in NOD-like receptors: An association study on risk and survival of colorectal cancer. *PLoS One.*2018, 13(6):e0199350.doi:10.1371/journal.pone.0199350.
30. Pei G, Dorhoi A. NOD-Like Receptors: Guardians of Cellular Homeostasis Perturbation during Infection. *Int J Mol Sci.*2021, 22(13).doi:10.3390/ijms22136714.

31. Wang H, Lin X, Pu X. NOD-like receptors mediate inflammatory lung injury during plateau hypoxia exposure. *J Physiol Anthropol.*2020, 39(1):32.doi:10.1186/s40101-020-00242-w.
32. Lupfer CR, Anand PK, Qi X et al. Editorial: Role of NOD-Like Receptors in Infectious and Immunological Diseases. *Front Immunol.*2020, 11:923.doi:10.3389/fimmu.2020.00923.
33. Wicherska-Pawłowska K, Wróbel T, Rybka J. Toll-Like Receptors (TLRs), NOD-Like Receptors (NLRs), and RIG-I-Like Receptors (RLRs) in Innate Immunity. TLRs, NLRs, and RLRs Ligands as Immunotherapeutic Agents for Hematopoietic Diseases. *Int J Mol Sci.*2021, 22(24).doi:10.3390/ijms222413397.
34. You MW, Kim D, Lee EH et al. The Roles of NOD-like Receptors in Innate Immunity in Otitis Media. *Int J Mol Sci.*2022, 23(4).doi:10.3390/ijms23042350.
35. Almeida-da-Silva CLC, Savio LEB, Coutinho-Silva R et al. The role of NOD-like receptors in innate immunity. *Front Immunol.*2023, 14:1122586.doi:10.3389/fimmu.2023.1122586.
36. Liu S, Fan W, Gao X et al. Estrogen receptor alpha regulates the Wnt/ β -catenin signaling pathway in colon cancer by targeting the NOD-like receptors. *Cell Signal.*2019, 61:86-92.doi:10.1016/j.cellsig.2019.05.009.
37. Poli G, Egidi MG, Cochetti G et al. Relationship between cellular and exosomal miRNAs targeting NOD-like receptors in bladder cancer: preliminary results. *Minerva Urol Nefrol.*2020, 72(2):207-213.doi:10.23736/S0393-2249.19.03297-1.
38. Sun G, Zheng C, Deng Z et al. TRAF5 promotes the occurrence and development of colon cancer via the activation of PI3K/AKT/NF- κ B signaling pathways. *J Biol Regul Homeost Agents.*2020, 34(4):1257-1268.doi:10.23812/19-520-A.
39. Xie Y, Li F, Li Z et al. miR-135a suppresses migration of gastric cancer cells by targeting TRAF5-mediated NF- κ B activation. *Onco Targets Ther.*2019, 12:975-984.doi:10.2147/OTT.S189976.
40. Chen Z, Zhao L, Zhao F et al. MicroRNA-26b regulates cancer proliferation migration and cell cycle transition by suppressing TRAF5 in esophageal squamous cell carcinoma. *Am J Transl Res.*2016, 8(5):1957-1970.
41. Xu C, Sui S, Shang Y et al. The landscape of immune cell infiltration and its clinical implications of pancreatic ductal adenocarcinoma. *J Adv Res.*2020, 24:139-148.doi:10.1016/j.jare.2020.03.009.
42. Kamal AM, El-Hefny NH, Hegab HM et al. Expression of thioredoxin-1 (TXN) and its relation with oxidative DNA damage and treatment outcome in adult AML and ALL: A comparative study. *Hematology.*2016, 21(10):567-575.doi:10.1080/10245332.2016.1173341.
43. Chutkow WA, Patwari P, Yoshioka J et al. Thioredoxin-interacting protein (Txnip) is a critical regulator of hepatic glucose production. *J Biol Chem.*2008, 283(4):2397-2406.doi:10.1074/jbc.M708169200.
44. Powis G, Kirkpatrick DL. Thioredoxin signaling as a target for cancer therapy. *Curr Opin Pharmacol.*2007, 7(4):392-397.doi:10.1016/j.coph.2007.04.003.
45. Welsh SJ, Bellamy WT, Briehl MM et al. The redox protein thioredoxin-1 (Trx-1) increases hypoxia-inducible factor 1 α protein expression: Trx-1 overexpression results in increased vascular endothelial growth factor production and enhanced tumor angiogenesis. *Cancer Res.*2002, 62(17):5089-5095.
46. Baker AF, Koh MY, Williams RR et al. Identification of thio redoxin-interacting protein 1 as a hypoxia-inducible factor 1 α lpha-induced gene in pancreatic cancer. *Pancreas.*2008, 36(2):178-186.doi:10.1097/MPA.0b013e31815929fe.
47. Ungerstedt JS, Sowa Y, Xu WS et al. Role of thioredoxin in the response of normal and transformed cells to histone deacetylase inhibitors. *Proc Natl Acad Sci U S A.*2005, 102(3):673-678.doi:10.1073/pnas.0408732102.
48. Grogan TM, Fenoglio-Prieser C, Zeheb R et al. Thioredoxin, a putative oncogene product, is overexpressed in gastric carcinoma and associated with increased proliferation and increased cell survival. *Hum Pathol.*2000, 31(4):475-481.doi:10.1053/hp.2000.6546.
49. Tonissen KF, Di Trapani G. Thioredoxin system inhibitors as mediators of apoptosis for cancer therapy. *Mol Nutr Food Res.*2009, 53(1):87-103.doi:10.1002/mnfr.200700492.

Conclusion:In summary, our findings suggest that cancer risk scores exhibit potential as independent prognostic factors. Additionally, TRAF5 may serve as a potential cancer marker. Effector memory CD8 T cells and Immature B cells demonstrate promise as viable drug targets to enhance patient survival. Moreover, TXN shows potential as a target for the development of cancer drugs.**Competing interests:**The authors declare that they have no known competing financial interests or personal relationships that could have appeared to influence the work reported in this paper.**Acknowledgements:**The authors would like to express their gratitude to all participants who participated in this study.**Author Contributions:**QXM: Conceptualization, Formal analysis, Writing - original draft, Writing - review & editing. TCQ: Data curation, Visualization, Writing - original draft. TYY: Methodology, Writing - original draft. ZJL, HLW, BX, BYL, WL, DZ, NLJ,HFW: Methodology, Data curation, Software, Visualization. WJL, YLH: Writing - review & editing, Funding acquisition. All authors have read and agreed to the published version of the manuscript.**Funding:**This work is supported by the National Natural Science Foundation of China (82160537), the Key Research and Development Program of Guangxi(Guik eAB22035027, Guik eAB24010148), and the National Key Research and Development Program of China(2023YFC2605400).**Data Availability:** All data were derived from the public databases (KEGG, TCGA and GEO). All R packages used are available online.**Ethics approval and consent to participate:**Not applicable.**Consent for publication:**Not applicable.